sciendo

TRANSACTIONS ON AEROSPACE RESEARCH
4(257) 2019, pp.66-80
DOI: 10.2478/tar-2019-0024
eISSN 2545-2835

COMPARATIVE ANALYSIS OF MACRO- AND MICROSTRUCTURE OF PRINTED ELEMENTS IN THE FDM, SLS AND MJ TECHNOLOGIES

Natalia Majca-Nowak, Ewelina Kluska, Piotr Gruda
Aviation Systems, Engineering Design Center,
Al. Krakowska 110/114, 02-256 Warsaw, Poland
Natalia.Majca@ge.com, ewelina.kluska@ge.com, piotr.gruda@ge.com

Abstract

The article presents research conducted with the project: 'Additive manufacturing in conduction with optical methods used for optimization of 3D models" [2]. The article begins with the description of properties of the materials used in three different additive technologies – Fused Deposition Modelling (FDM), Selective Laser Sintering (SLS) and Material Jetting (MJ). The next part focuses on the comparative analysis of macro- and microstructure of specimens printed in order to test selected materials in additive technologies mentioned above. In this research two types of specimens were used: dumbbell specimens and rectangular prism with hole specimens. In order to observe macrostructure specimens, they were subjected to load test until it broke. In the case of observing microstructure, they were cut in some places. Each of described additive technologies characterizes by both different way of printing and used materials. These variables have a significant influence on macro- and microstructure and fracture appearance. FDM technology specimens printed of ABS material characterized by texture surface appearance. SLS technology specimens printed of PA12 material characterized by amorphous structure. MJ technology specimens printed of VeroWhite Plus material characterized by fracture appearance which had quasi- fatigue features. The microstructure of these specimens was uniform with visible inclusions.

Keywords: additive manufacturing, 3D printing, macrostructure, microstructure, FDM, SLS, MJ, PolyJet.

1. INTRODUCTION

The purpose of this article is to recognize macro- and microstructure of selected both 3D printing technologies and materials which are described in [1], [2]. It is suspected that the 3D printing process can create a different structure and material behaviour during load than other technologies. There were chosen three technologies: FDM, SLS and MJ. These technologies were selected considering literature and information contained in manufacturer brochures. The revision was created analyses of complicated shapes by the best parameters for each 3D printing method for the accessible printing machines. Some reference specimens were printed in above technologies to show specimens macrostructure after load test and microstructure of non-damaged specimens.

2. 3D PRINTING TECHNOLOGIES – MATERIALS SPECIFICATION

2.1. FDM technology – ABS material specification

The FDM (Fused Deposition Modelling) method uses ABS thermoplastic material as a built material. Considering information from [3], [11] ABS material is characterized by amorphous structure composed of three monomers: acrylonitrile, butadiene and styrene. The main attributes of ABS are its impact resistance and toughness. Article [14] described research on ABS resin with some rubber inclusions. The article [6] contains information about rapid prototyping manufacturing process of ABS material and how a layer thickness influenced accuracy of model. Extrusion is a standard method for ABS production. It can be observed [8], that cross-section of extruded ABS material consists of incomplete bonding between lines of extruded material (see Figure 1). The ABS fracture microstructure obtained under static load was examined by SEM (scanning electron microscope) in Figure 2 and revealed stress whitened and fibrillated structure. The massive cavitation inside the rubbery particles and in the boundary between the matrix and inclusions were observed.

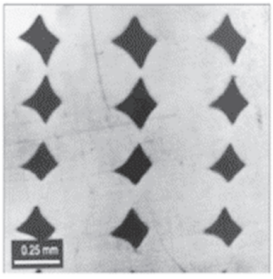

Figure 1. Standard macrostructure for FDM-ABS material built by extrusion process [8]

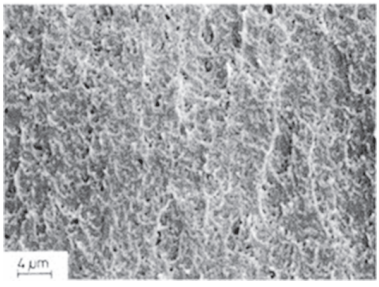

Figure 2. Fracture surface micrographs of ABS sample under static conditions [14]

2.2 SLS technology – PA12 material specification

The main limiting SLS (Selective Laser Sintering) technology for wide-range industrial scope is the narrow variety of applicable polymers [4]. The paper [5] informs that SLS produced parts are affected by the layer structure and printing settings hence mechanical performance of 3D elements is different than those produced in a conventional way (i.e. injection molding). PA12 and its dry blended mixes are ca. 90% of industrial production. Microstructural observations of HT PA12 powder gathered by [12] revealed unmelted grains and spherulites surrounding them (see Figure 3 marked on red). There were also detected irregular shaped pores with residual air (see Figure 4). Similar observations were carried out in another article [7] regarding 3D printed PA12 material (see Figure 5).

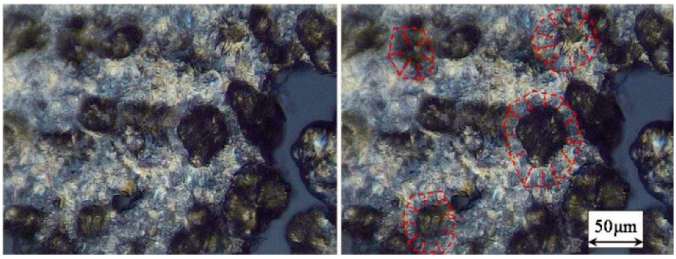

Figure 3. Polarized optical transmission microscope (TEM) micrograph of an HT processed PA12 [12]

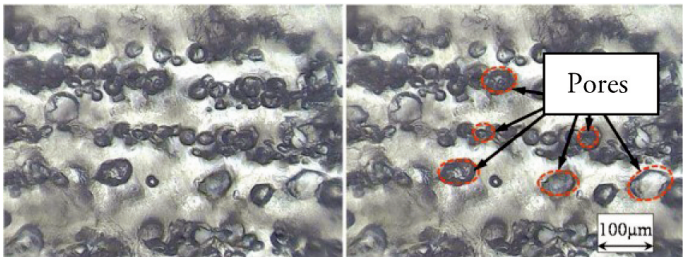

Figure 4. Optical micrograph of an excessively exposed PA12 [12]

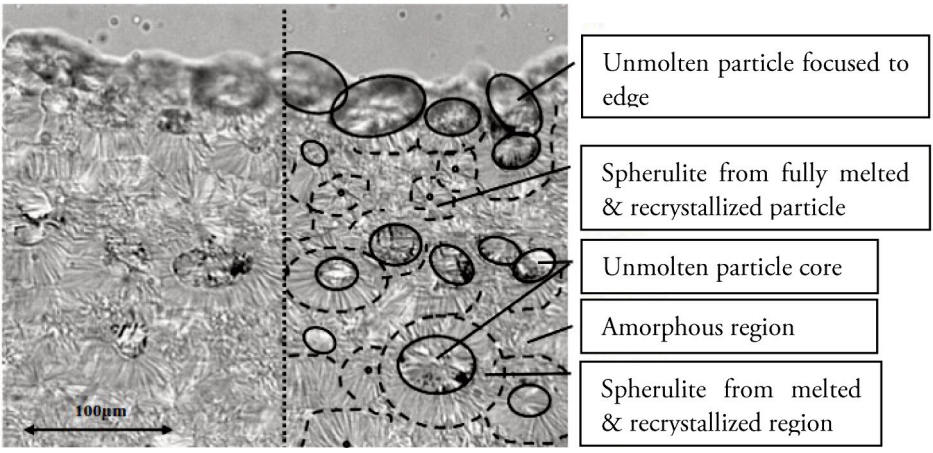

Figure 5. Microstructure of SLS PA12 material [7]

2.3. Material Jetting technology VeroWhite Plus material specification

The base material for the MJ (Material Jetting) is VeroWhite Plus acrylic resin. Article [10] consists of information about microstructure of heat cure and cold cure acrylic resin. The microstructure observed using SEM after conventional fabrication technique was smooth and homogenous while vacuum casting fabricated technique produced the same resin with pores what required additional degassing. Fracture of acrylic resin has brittle appearance.

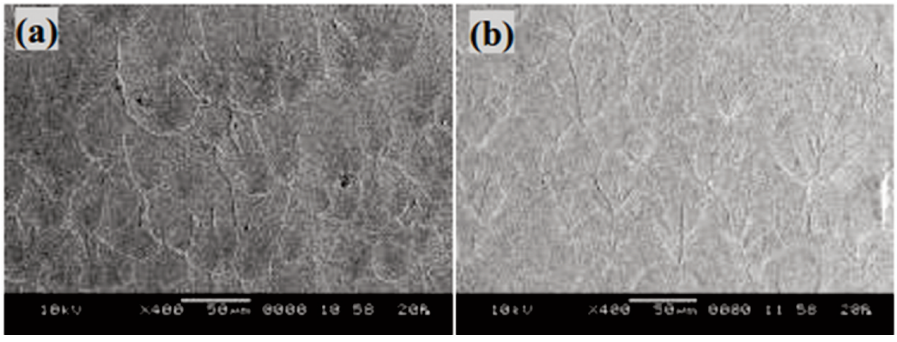

Figure 6. SEM of fracture specimens (x400 mag): (a) conventional technique heat cure resin; (b) conventional technique cold cure resin [10]

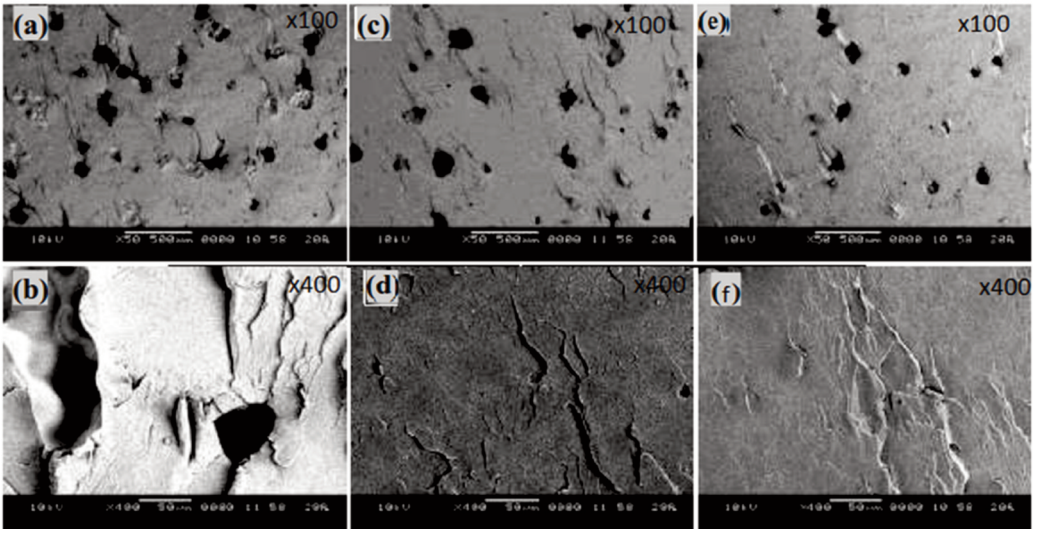

Figure 7. SEM of vacuum casting technique heat cold cure resin fracture specimens:
(a)-(b) no degassing; (c)-(d) 20 sec degassing; (e)-(f) 40 sec degassing [10]

3. COMPARISON OF MACRO- AND MICROSTRUCTURE

Each observation was conducted on three specimens from the same printing process. The first material was ABSplus-P430 from FDM technology, the second one was VeroWhite Plus from MJ technology and the last one was Polyamide12 from SLS technology. Two different specimens' shapes: dumbbell specimens and rectangular prism with hole specimens were prepared to verify macro- and microstructure of 3D printing methods.

Macrostructure was observed on dumbbell specimens (see Figure 8) and rectangular prism with hole specimens (see Figure 9) which were subjected to the load test. Broken specimens should show the type and privilege way of cracking. Furthermore, it should present the weakest point of the observed technology when it is under load.

Microstructure was observed on a rectangular prism with hole specimens. These specimens were cut and observed in three different directions without any load test on them. They were cut slowly using diamond saw in three different places to observe internal structure on a cross section (see Figure 9, blue line with point a).

Front and profile (see Figure 9) of the specimens were observed to see the full three-dimensional view of structure. All specimens were printed as material-filled elements.

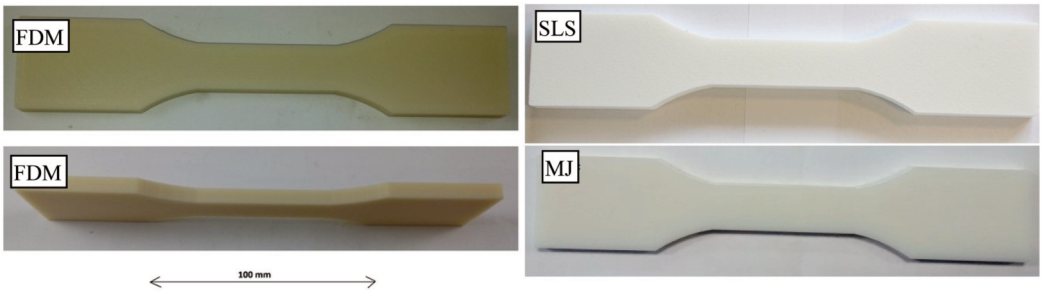

Figure 8. Printed dumbbell specimens prepared for mechanical test and macrostructure observation

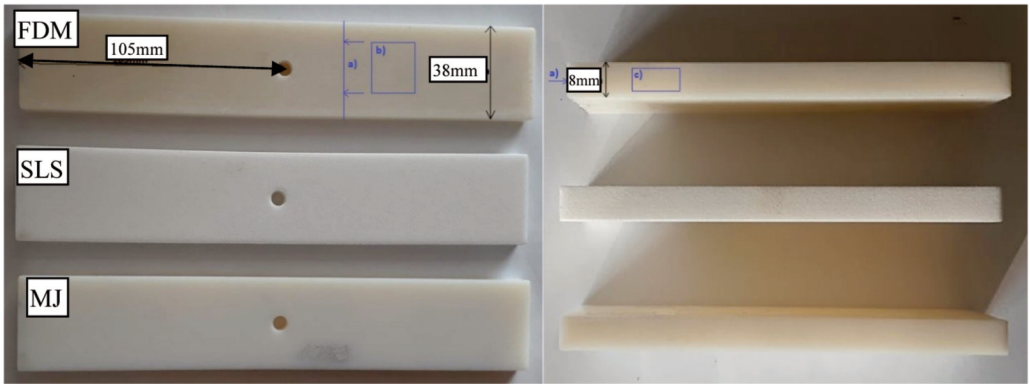

Figure 9. Printed rectangular prism with hole specimens prepared for macro- and microstructure observation

3.1. FDM technology

First step was to test specimens in the FDM technology. Reference specimens were printed on the Fortus 250mc machine produced by the Stratasys company. Three dumbbell specimens and three rectangular prism specimens with hole were printed and subjected to load test until it broke. The maximum achieved load was 3.54 kN. The specimen breaks at tensile strength 21.7 MPa and the elongation at break achieved 1.82%. Young modulus reached 1994 MPa.

Figure 10 presents dumbbell FDM specimen after the break. Naked eye observations revealed crossed bands on the specimen surface. The specimen breaks creating both sharp and rough edges. Fracture macrostructure observations revealed bands and layers visible inside the specimen.

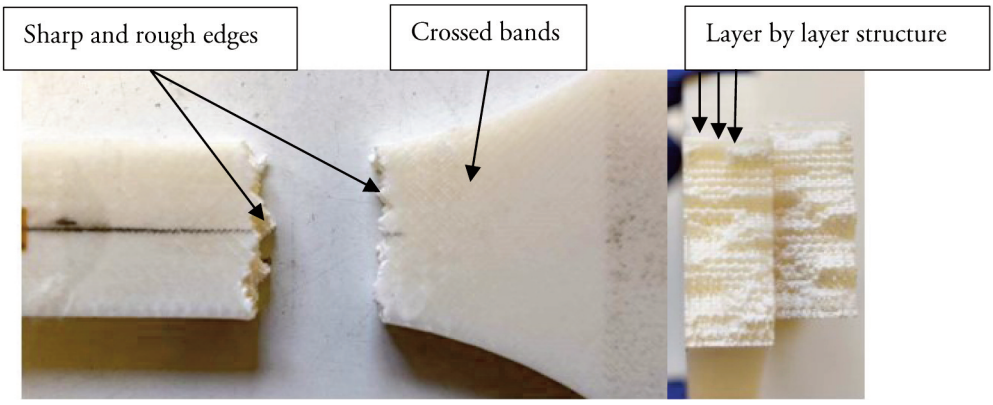

Figure 10. FDM dumbbell specimen with visible macrostructure after the break

Figure 11 presents rectangular prism with hole specimen after the break. Naked eye observations of two specimens revealed that crack went as expected with one exception – the hole in the middle of specimen stayed unharmed. The crack goes between hole and the next layer. The reason of this type of break can be printing manner which created a hole as a circle from one, individual layer. Figure 12 and Figure 13 present a regular crack of rectangular prism with hole specimens. Regular direction of crack propagation which reached 90° angle was noticed.

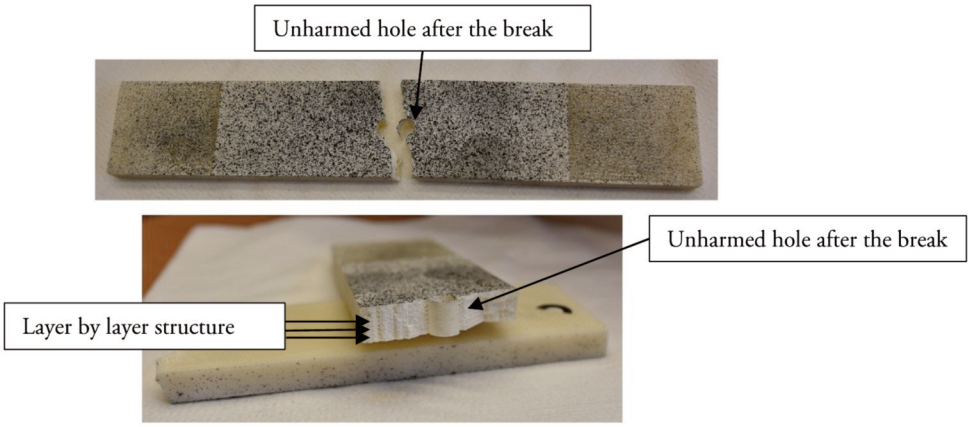

Figure 11. FDM rectangular prism with hole specimen with visible macrostructure and unharmed hole after the break

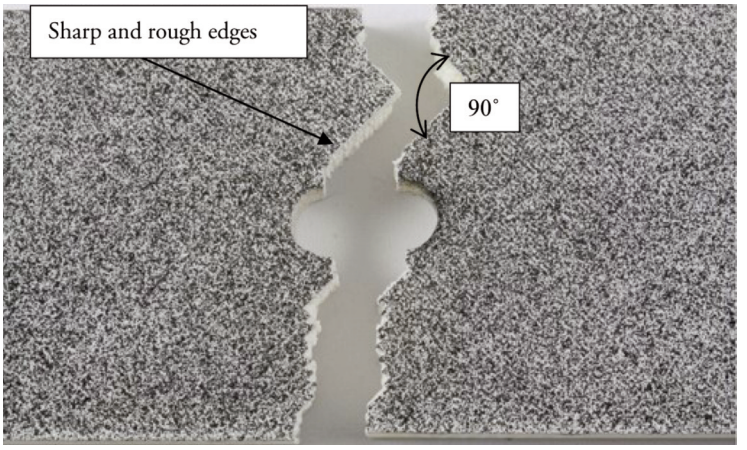

Figure 12. FDM rectangular prism with hole specimen with visible macrostructure after the break, sharp and rough edges

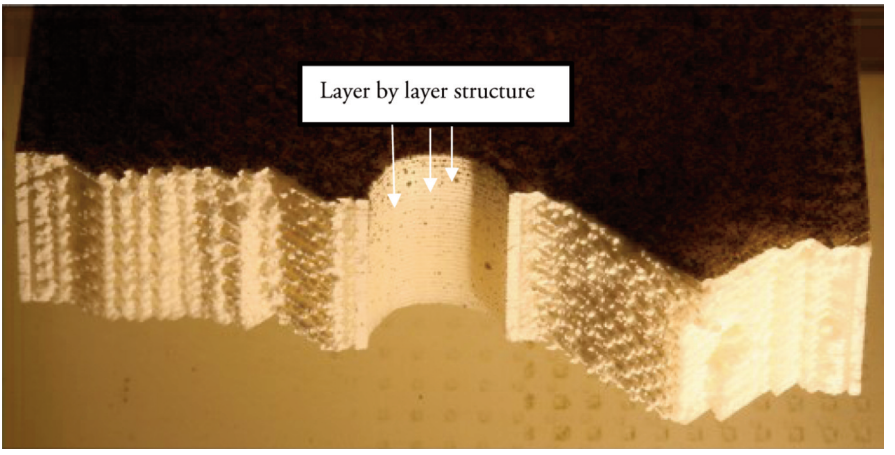

Figure 13. FDM rectangular prism with hole specimen with visible macrostructure after the break, layer by layer structure

Afterwards, microstructure was checked on the rectangular prism with hole specimens. Cross section observations (see Figure 14) revealed that ABS layers were printed with noticeable shift what gave waved spaces between these layers. The layer thickness was generally similar in each location so the layers shift in Z axis could be the result of printer inaccuracy. The front surface observations (see Figure 15) revealed that structure was built using layers with 90° angle between them what have created crossed layers view. They were built one by one in Z axis (see Figure 16).

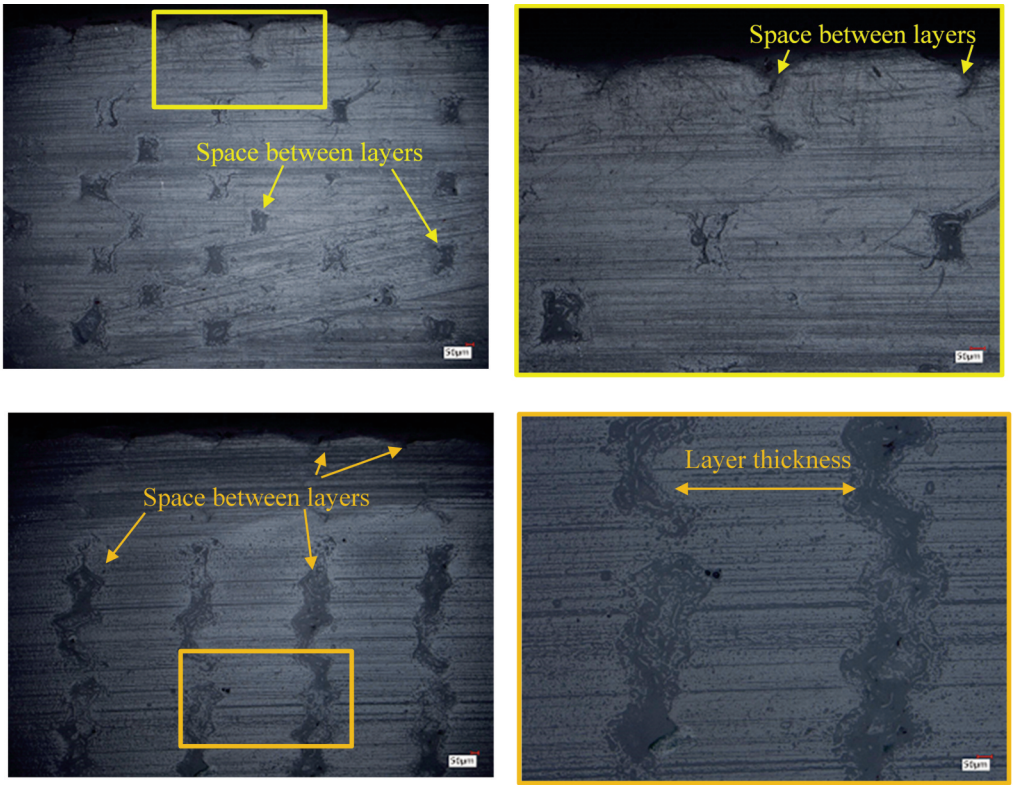

Figure 14. FDM rectangular prism with hole cross section microstructure view (see Figure 9). Pictures with magnification x100 and x200

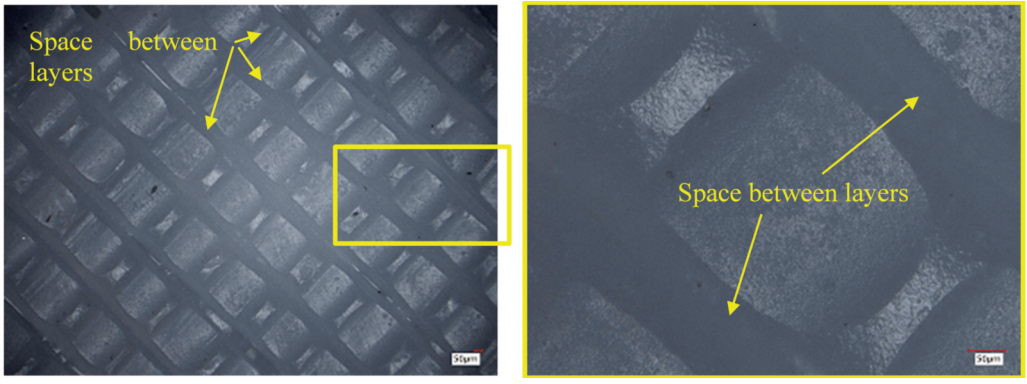

Figure 15. FDM rectangular prism with hole front microstructure view (see Figure 9). Pictures with magnification x100 and x500

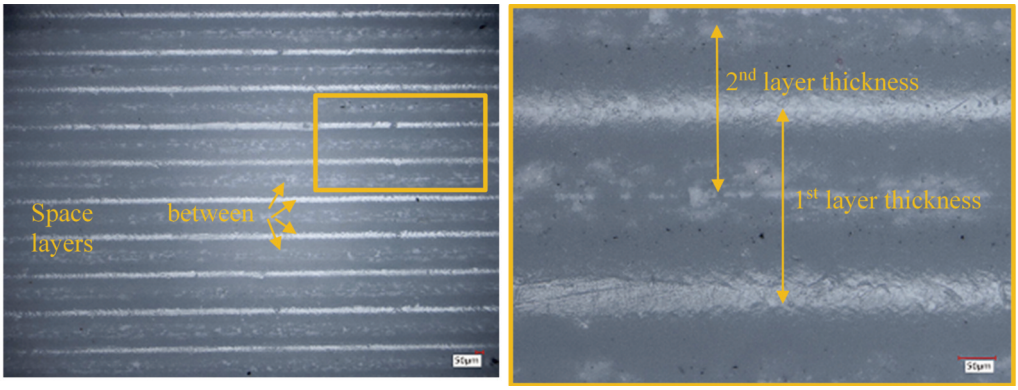

Figure16. FDM rectangular prism with hole profile microstructure view (see Figure 9c). Pictures with magnification x100 and x500

3.2. SLS technology

The second step was to test specimens in the SLS technology. Reference specimens were printed on the EOSINT P 395 machine produced by EOS company. Three dumbbell specimens and three rectangular prism specimens with hole were printed and subjected to load test until it broke. The maximum achieved load was 8.03 kN. The specimen breaks at tensile strength 49.1 MPa and the elongation at break achieved 9.00%. Young modulus reached 2147 MPa.

Figure 17 presents the dumbbell SLS specimen after the break. Naked eye observations revealed that material crumbed during the load test and as a result some material chips were created. Slightly rough fracture appearance which consisted of randomly pulled out powder grains was noticed as well (see Figure 18).

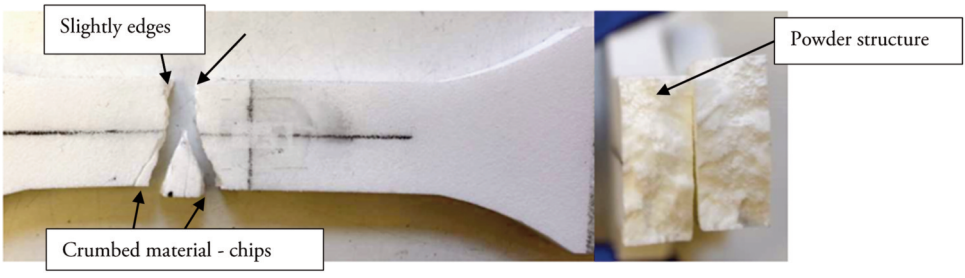

Figure 17. SLS dumbbell specimen with visible macrostructure after the break

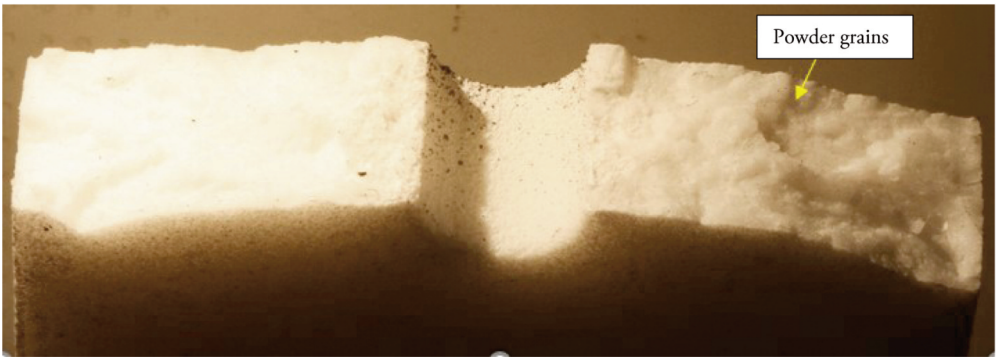

Figure 18. SLS rectangular prism with hole specimen with visible macrostructure after the break

Afterwards, microstructure was checked on a rectangular prism with hole specimens. Cross section observations (see Figure 19) revealed some empty holes from where PA12 material grains were pulled off during cut. The front and profile microstructures are similar (see Figure 20 and Figure 21) and can be described as amorphous. The reason of this similarity and microstructure type is the printing manner, where element is printed in the space filled randomly with the powder. The powder grains are well visible during observations because SLS technology sinter powder grains instead of melting them together.

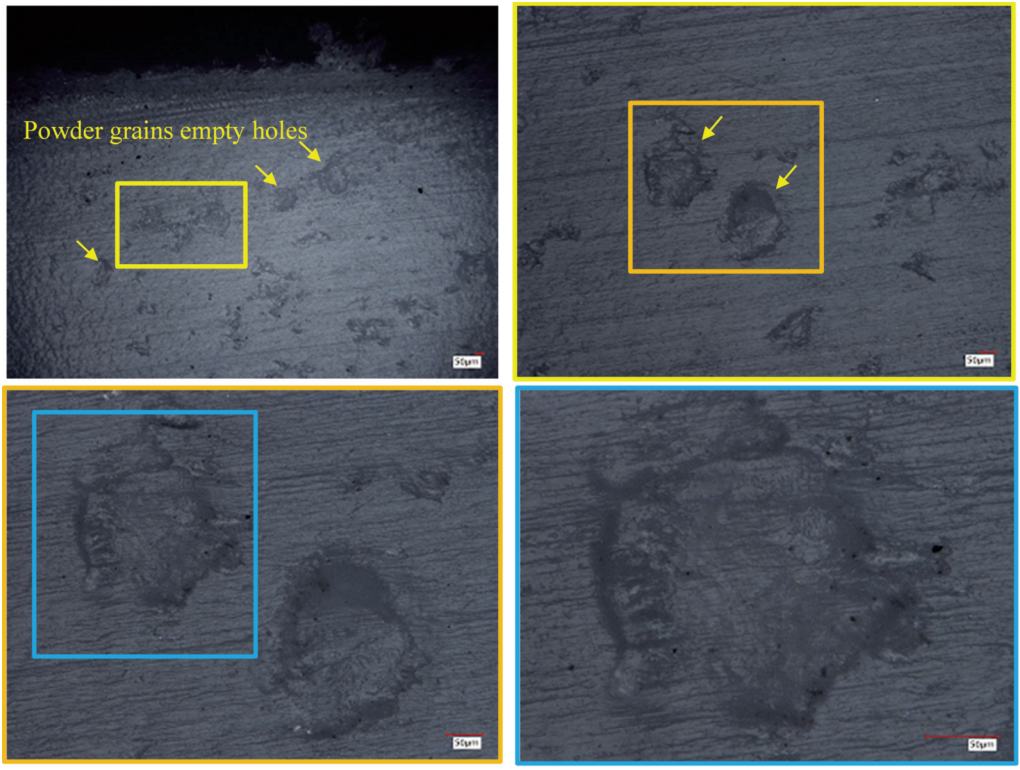

Figure 19. SLS rectangular prism with hole cross section microstructure view (see Figure 9).
Pictures with magnification x100, x200, x500 and x1000

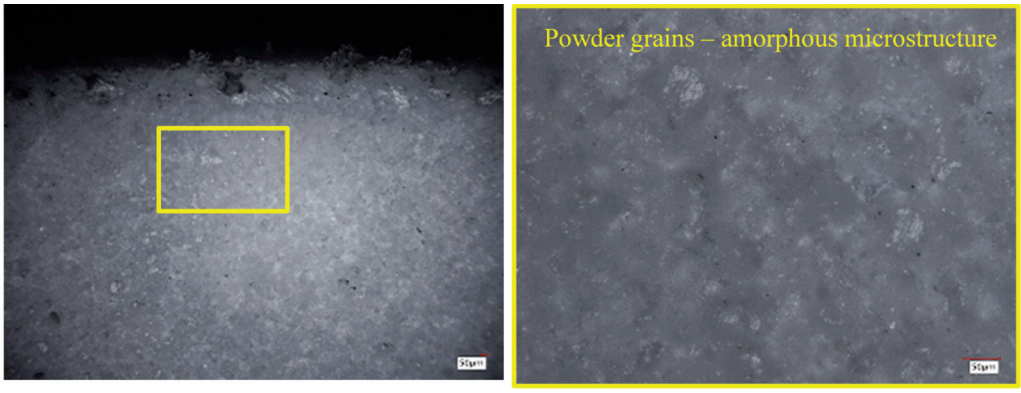

Figure 20. SLS rectangular prism with hole front microstructure view (see Figure 9).
Pictures with magnification x100 and x500

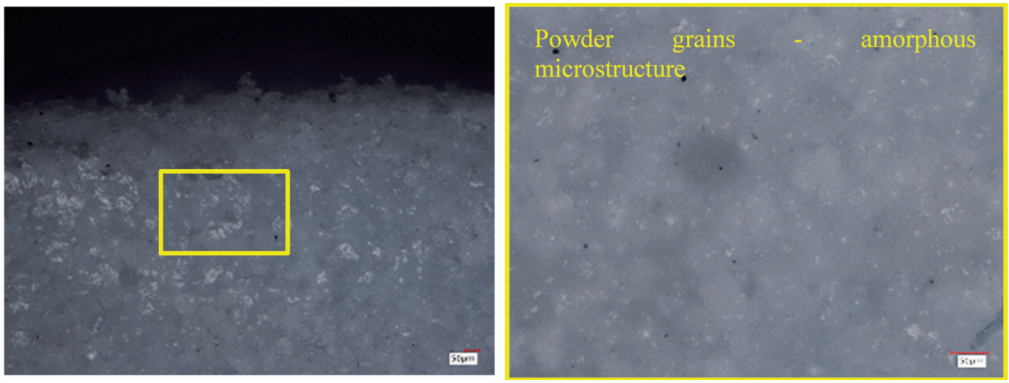

Figure 21. SLS rectangular prism with hole profile microstructure view (see Figure 9). Pictures with magnification x100 and x500

3.3. Material Jetting technology (PolyJet method)

The last step was to test flat and three-dimensional specimens in the Material Jetting technology. Reference specimens were printed in PolyJet method on the Objet 30 Prime machine produced by Stratasys company. Three dumbbell specimens and three rectangular prism specimens with a hole were printed and subjected to load test until it broke. The maximum achieved load was 7.73 kN. The specimen breaks at tensile strength 48.4 MPa and the elongation at break achieved 5.14%. Young modulus reached 2695 MPa.

Figure 22 presents dumbbell PolyJet specimen after the break. Naked eye observations revealed smooth and straight crack edges. Close fracture observations (see Figure 23, Figure 24 and Figure 25) allowed to notice quasi-fatigue fracture behaviour. Crack origin located on the hole edges and quasi-striations which suggest crack propagation direction was noticed. Moreover, fracture was characterized by cleavage appearance what is common feature of brittle materials.

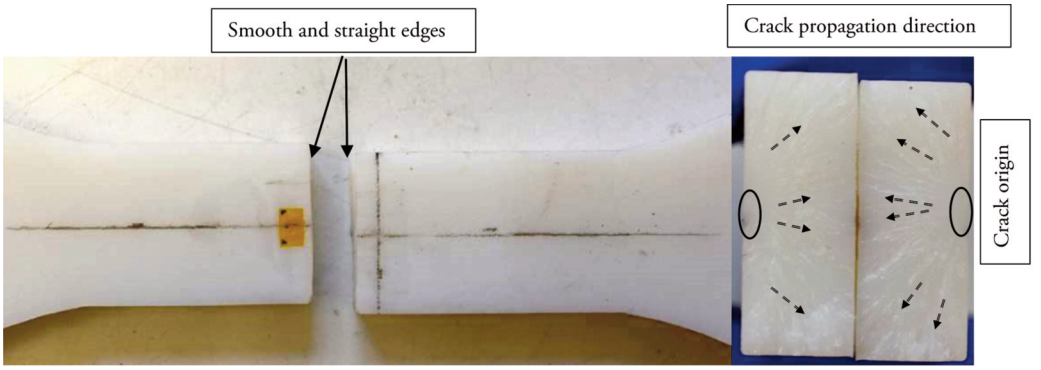

Figure 22. PolyJet dumbbell specimen with visible macrostructure after the break

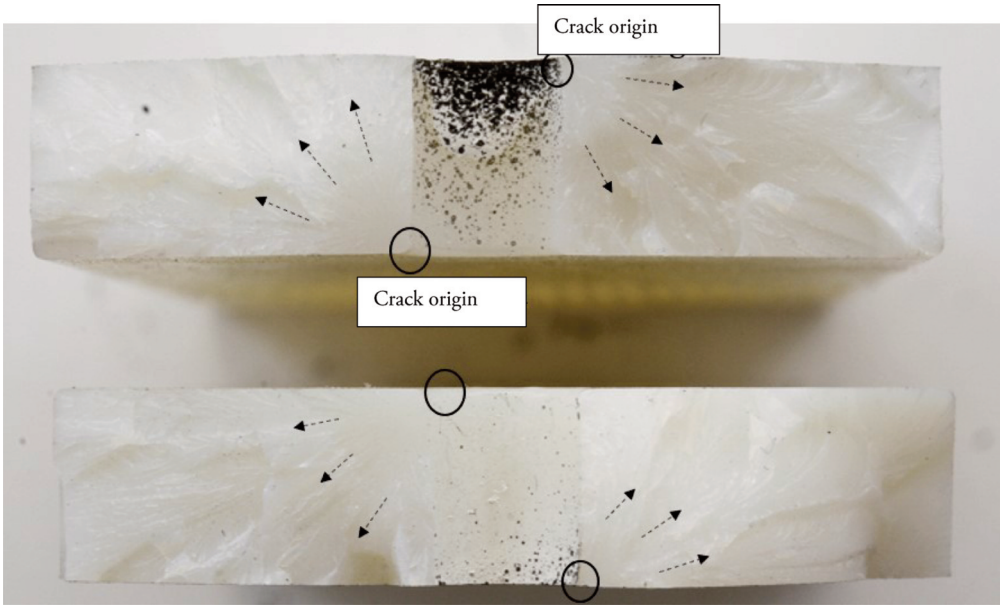

Figure 23. PolyJet rectangular prism with hole specimen with visible macrostructure after the break, crack origin

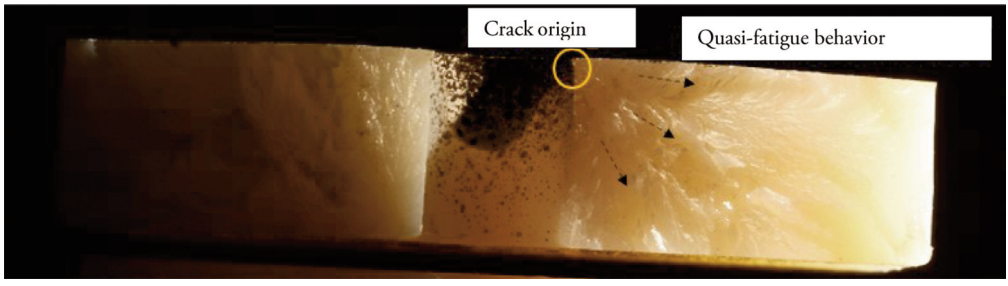

Figure 24. PolyJet rectangular prism with hole specimen with visible macrostructure after the break, quasi-fatigue behaviour

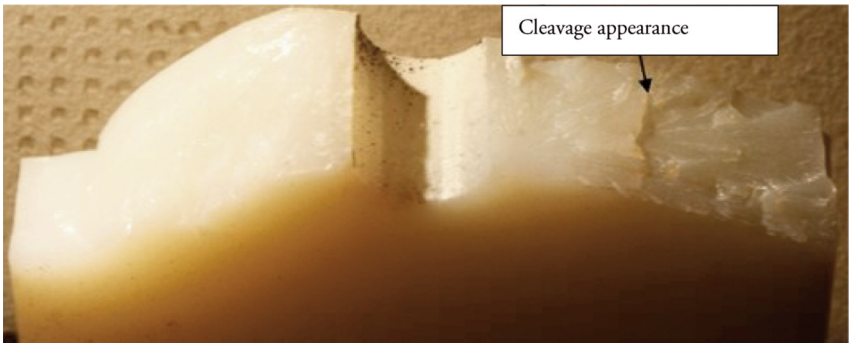

Figure 25. PolyJet rectangular prism with hole specimen with visible macrostructure after the break, cleavage appearance

Afterwards, microstructure was checked on a rectangular prism with hole specimens. Cross section observations (Figure 26) revealed uniform microstructure with some impurities. Structure is uniform also on a front surface (Figure 27) because drops are melted together during the printing process what avoids empty spaces creation between them. The profile microstructure view (Figure 28) is consisted of multi-layer structure which is characterized by bands built of packages of layers in different directions. The layer thickness was 28μm whereas one package of layers (one band) was ca. 400μm.

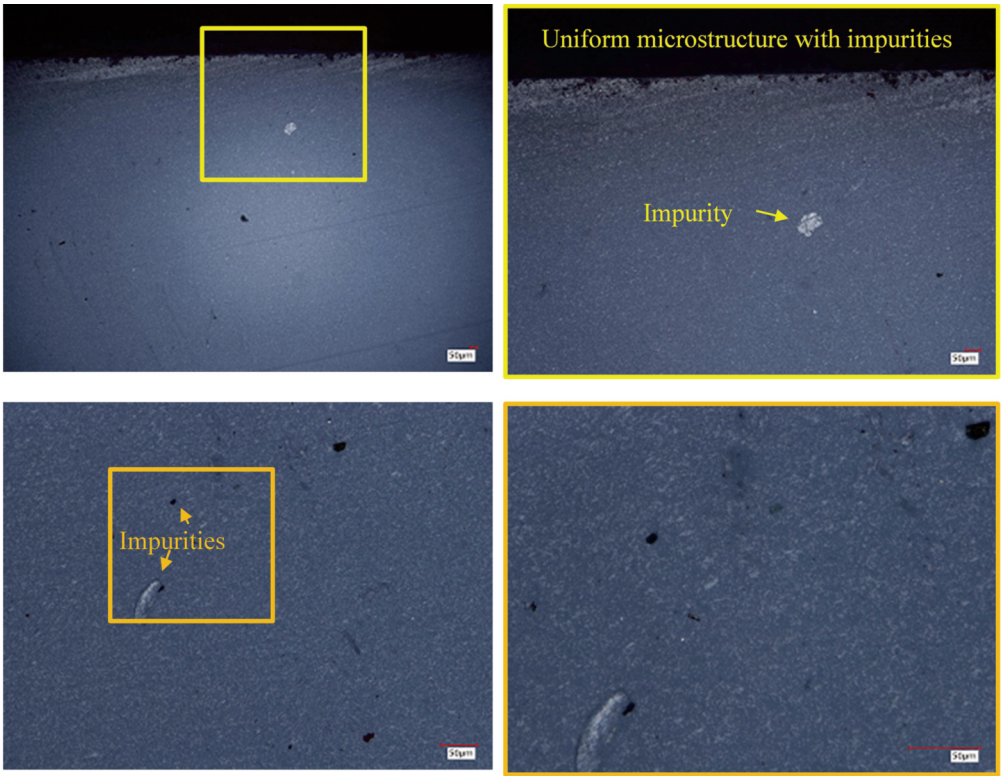

Figure 26. PolyJet rectangular prism with hole cross section microstructure view (see Figure 9a). Pictures with magnification x100, x200, x500 and x1000

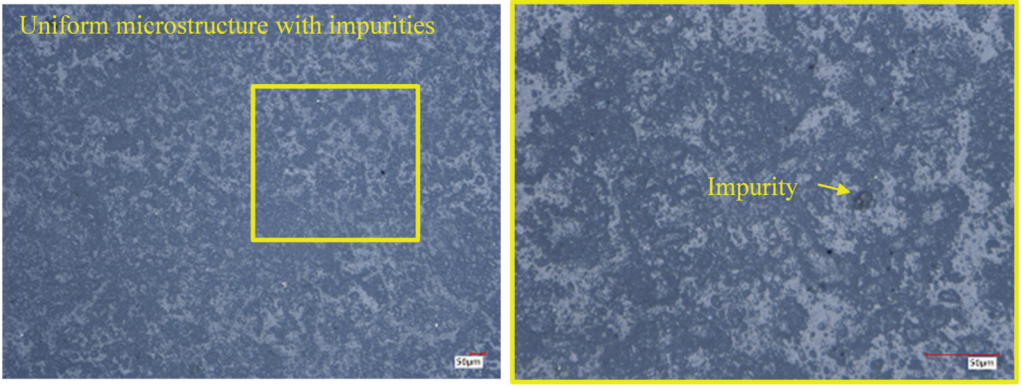

Figure 27. PolyJet rectangular prism with hole front microstructure view (see Figure 9b). Pictures with magnification x200 and x1000

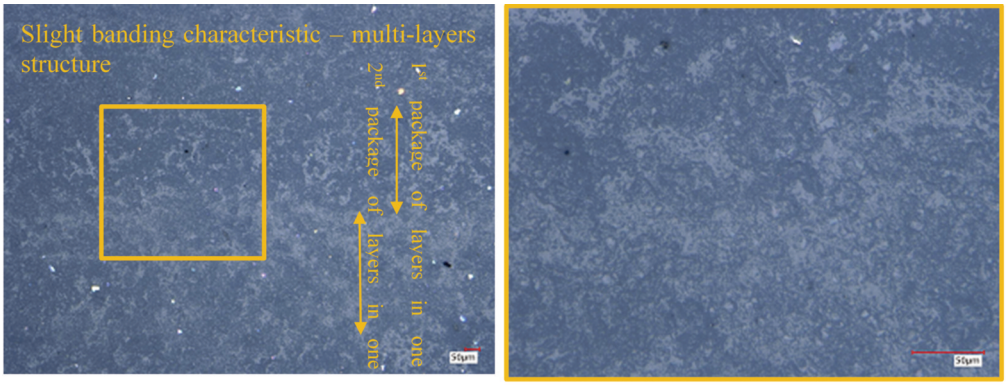

Figure 28. PolyJet rectangular prism with hole profile microstructure view (see Figure 9c). Pictures with magnification x200 and x1000

4. SUMMARIZE

The main purpose of this article was the comparative analysis of macro- and microstructure of three different additive technologies - Fused Deposition Modelling (FDM), Selective Laser Sintering (SLS) and Material Jetting (MJ). In this research two types of specimens were used: dumbbell specimens and rectangular prism with hole specimens. In order to observe macrostructure specimens, they were subjected to load test until it broke. In the case of observing microstructure, they were cut in some places. Each of described additive technologies characterizes by both different way of printing and used materials. These variables have a significant influence on macro- and microstructure and fracture appearance.

For FDM technology specimens printed of ABS material, macrostructure observations revealed crossed bands (90° angle) on the specimen surface with both sharp and rough edges near the fracture. The printing manner had a huge influence on the fracture shape. The fracture consisted of bands and layers due to which the crack propagation direction was changed each 90˚angle. Furthermore, crack went through the specimen leaving a hole in the middle of specimen unharmed - this hole was printed as a circle from one, individual layer, due to that the privileged cracking path was between the layers. Microstructure cross section observations revealed that ABS layers were printed with noticeable shift what gave waved spaces between these layers. The layer thickness was generally similar in each location, so the layers shift in Z axis could be the result of printer inaccuracy.

For SLS technology specimens printed of PA12 material, macrostructure observations revealed that material crumbed during the load test and as a result some material chips were created. Slightly rough fracture appearance which consisted of randomly pulled out powder grains, was also noticed. The powder grains were well visible during observations because SLS technology sinter powder grains instead of melting them together. Microstructure cross section observations confirmed some empty holes from where PA12 material grains were pulled off. The microstructure was amorphous due to the printing manner where elements were printed in the space filled randomly with the powder.

For MJ technology specimens printed of VeroWhite Plus material (PolyJet method), macrostructure observations revealed smooth and straight crack edges. Fracture was characterized by cleavage appearance what is common feature of brittle materials. Close observations allowed to notice fracture appearance which had quasi-fatigue features.

Crack origin located on the hole edges and quasi-striations which suggested crack propagation direction, was noticed. Microstructure observations revealed uniform microstructure with some impurities. Uniform structure was achieved because drops were melted together during the printing process what avoids empty spaces creation between them. The microstructure profile view revealed

multi-layer structure which was characterized by bands built of packages of the layers in different directions. The layer thickness was 28μm whereas one package of layers (one band) was ca. 400μm.

BIBLIOGRAPHY

[1] Kluska E., Gruda P., Majca-Nowak N. The accuracy and the printing resolution comparison of different 3D printing technologies. Warsaw: Institute of Aviation, 2019.
[2] Kluska E., Gruda P., Majca-Nowak N. Additive manufacturing in conduction with optical methods used for optimization of 3D models. Warsaw: Institute of Aviation, 2018.
[3] Vishwakarma S., Pandey P., Gupta N. Characterization of ABS material: Review. Journal of Research in Mechanical Engineering. 5, 2017, Vol. 3, pages 13-16.
[4] Lammens N., De Baere I., Van Paepegem W. On the orthotropic elasto-plastic material response of additively manufactured polyamide 12. Zwijnaarde, Belgium: Ghen University, 2017.
[5] Schmid M., Amado A., Wegener K. Polymer powders for Selective Laser Sintering (SLS). Switzerland : API Conference - American Institute of Physics, 2015. Volume 1664.
[6] Hafsa M., Ibrahim M., Wahab M., Zahid M. Evaluation of FDM pattern with ABS and PLA material. Applied Mechanics and Materials. 2013, Vols. 465-466, pages 55-59.
[7] Niino T., Haraguchi H., Itagaki Y. Microstructural observation and mechanical property evaluation of plastic parts obtained by preheat free laser sintering. Japan: Institute of Industrial Science - Tokyo University, August 2012.
[8] Kassim N, Saidin Wahab M, Yusof Y. Bali Physical properties and fracture surface of acrylic denture bases processed by conventional and vacuum casting fabrication technique. 12th International Conference on QiR (Quality in Research), 2011. ISSN 114-1284.
[9] Bourell D., Leu M., Rosen D. Rodamap for Additive Manufacturing: Identifying the Future of Freeform Processing. Austin: Tech Rep, 2009.
[10] Zarringhalam H., Hopkinson N., Kamperman N.F., de Vlieger J.J. Effects of processing on microstructure and properties of SLS nylon 12. United Kingdom: Loughborough University, 2008.
[11] ABS-acrylonitrile butadiene styrene. [Online] 2003. http://designinsite.dk/htmsider/m0007.htm.
[12] M., Stocker. From Rapid Prototyping to Rapid Manufacturing. Auto Technology. 2002, Vol. 2, pages 38-40.
[13] Rodriguez J., Thomas J., Renaud J. Characterization of the mesostructure of styrene materials. Rapid Prototyping Journal. 3, 2000, Vol. 6, pages 175-185.
[14] Bernal C., Frontini P., Sforza M., Bibbo M. Microstructure, Deformation, and Fracture Behavior of Commercial ABS Resins. Journal of Applied Polymer Science. DOI: 10.1002/app.1995.070580101, October 1995.

ANALIZA PORÓWNAWCZA MAKRO- I MIKROSTRUKTURY DRUKOWANYCH ELEMENTÓW 3D W TECHNOLOGIACH FDM, SLS ORAZ MJ

Streszczenie

Niniejszy artykuł prezentuje wyniki testów, które powstały w trakcie realizacji projektu „Addytywne wytwarzanie w połączeniu z metodami optycznymi stosowane do optymalizacjii modeli przestrzennych”(2). Artykuł rozpoczyna się opisem właściwości materiałów użytych w trzech wybranych

technologiach przyrostowych – Fused Deposition Modeling (FDM), Selective Laser Sintering (SLS) oraz Material Jetting (MJ). W dalszej części dokonano analizy porównawczej makrostruktury oraz mikrostruktury dla próbek referencyjnych wydrukowanych na potrzeby testu z wyselkcjonowanych materiałów w podanych technologiach przyrostowych. Ze względu na rodzaj obserwacji, w badaniach użyto dwóch rodzajów próbek: próbki wiosełkowe oraz płaskie, prostokątne próbki z otworem. W celu obserwacji makrostruktury próbki poddane zostały obciążeniu aż do zerwania. Natomiast, w celu obserwacji mikrostruktury zostały pocięte w kilku miejscach. Każda z opisanych w tym artykule technologii przyrostowych charakteryzuje się innym sposobem drukowania oraz zastosowanym materiałem. Zmienne te mają znaczący wpływ na makrostrukturę, mikrostrukturę oraz przełom. Próbki wydrukowane z materiału ABS w technologii FDM charakteryzują się widoczną teksturą materiału. Próbki wydrukowane z PA12 w technologii SLS charakteryzują się strukturą amorficzną. Charakterystyczny dla próbek wydrukowanych z VeroWhite Plus w technologii MJ był przełom, który miał cechy pseudo-zmęczeniowe. Mikrostruktura tych próbek była jednorodna z widocznymi wtrąceniami.

Słowa kluczowe: technologia przyrostowa, drukowanie 3D, mikrostruktura, makrostruktura, FDM, SLS, MJ, PolyJet.